Electronic Structure of Strongly Correlated Systems Emerging from Combining Path-Integral Renormalization Group with the Density-Functional Approach

Yoshiki Imai, Igor Solovyev, and Masatoshi Imada

Institute for Solid State Physics, University of Tokyo, Kashiwanoha, Kashiwa, Chiba, 277-8581, Japan and PRESTO, Japan Science and Technology Agency, 4-1-8 Honcho, Kawaguchi, Saitama, Japan

(Received 4 February 2005; published 19 October 2005)

A new scheme of first-principles computation for strongly correlated electron systems is proposed. This scheme starts from the local-density approximation (LDA) at high-energy band structure, while the low-energy effective Hamiltonian is constructed by a downfolding procedure using combinations of the constrained-LDA and the GW method. The obtained low-energy Hamiltonian is solved by the path-integral renormalization-group method, where spatial and dynamical fluctuations are fully considered. An application to Sr_2VO_4 shows that the scheme is powerful in agreement with experimental results. It further predicts a nontrivial orbital-stripe order.

DOI: 10.1103/PhysRevLett.95.176405 PACS numbers: 71.15.−m, 71.10.Fd, 71.30.+h

First-principles methods for electronic structure calculations have been extensively applied to various systems in the last few decades. The density-functional theory (DFT) supplemented with the local-density-approximation (LDA) [1,2], is one of the most successful schemes. However, in strongly correlated electron systems such as transition-metal oxides, LDA fails even at qualitative levels of simple systems and remain challenges in terms of first-principles calculations. The failure is ascribed to the correlation effects generating large spatial and dynamical fluctuations beyond the applicability of existing schemes.

In electronic structure calculations, DFT and wave function methods are two typical approaches [3]. The rapid development and recent extensive applications of the DFT approach rely on its less computation time while a systematic improvement of its accuracy is not an easy task. On the other hand, the wave function methods including the Hartree-Fock and variational schemes cost much longer computational time, while it offers a better accuracy for strongly correlated systems as we discuss later.

After considering this contrast, an optimal choice would be a hybrid method. Since the electrons far from the Fermi level do not show serious fluctuation effects, LDA and its self-energy correction called the GW approximation (GW) [4,5] offer a reasonable and efficient scheme there. If the elimination of the high-energy degrees of freedom by a downfolding scheme would result in the effective low-energy Lagrangian or Hamiltonian, they can be treated by an accurate wave function method. Such successive eliminations of the high-energy part have a conceptual similarity to the renormalization-group method. In this Letter, we propose a downfolding scheme to derive the low-energy effective models from the higher-energy structure, together with a reliable low-energy solver for the downfolded effective model, as a single framework of a first-principles method. To show the performance, we apply the present scheme to Sr_2VO_4, which reveals intriguing properties.

Since the electrons have kinetic and interaction energies, the downfolding procedure basically consists of two parts. One is to derive the screened Coulomb interaction after eliminating the high-energy degrees of freedom. The other is to take into account the effect on the kinetic part, as the self-energy effect from the high-energy electrons.

After eliminating the high-energy part, the effective model in general has a frequency dependence represented by a Lagrangian. However, in the low-energy region, the Hamiltonian approach, obtained by replacing the dynamical Coulomb interaction with the static one, still offers an efficient and essentially correct framework [6,7].

Recently, the dynamical mean-field theory (DMFT) [8] was employed as a low-energy solver for finite temperature properties [9]. Since the DMFT ignores the spatial correlations, its refinements by using the cluster or cellular algorithms [10,11] were attempted. In this Letter, we alternatively solve the low-energy effective Hamiltonian by the path-integral renormalization-group (PIRG) method [12] implemented with the quantum-number projection algorithm [13]. The PIRG scheme allows treating equally the spatial and dynamical fluctuations in a controllable way and hence makes it possible to obtain the ground state of the effective Hamiltonian exactly.

We now start with the downfolding procedure. We first perform the LDA calculations using the linear muffin-tin orbital (LMTO) method [14]. In many correlated electron systems, the bands close to the Fermi level are relatively well separated from the high-energy bands as in transition-metal oxides, where the bands near the Fermi level mainly consist of $3d$ character of transition-metal atomic orbitals (and frequently hybridized with oxygen $2p$ atomic orbitals). In this circumstance, the whole band may be downfolded to an effective model consisting only of the $3d$ bands (or additionally with the oxygen $2p$ bands). If the crystal field is strong, it may be downfolded even to the bands closest to the Fermi level, for example, the t_{2g} or e_g bands only, in a cubic environment. Here

we report the first attempt of the downfolding along this line.

When we restrict the degrees of freedom to the isolated LDA bands closest to the Fermi level, we first need to reduce the Hilbert space. With the notation for the states having the maximal weight near the Fermi level as $\{|d\rangle\}$ and the rest of the basis functions as $\{|r\rangle\}$, the whole Hilbert space may be spanned as $\{|\chi\rangle\} = \{|d\rangle\} \oplus \{|r\rangle\}$. A typical example of Sr_2VO_4 is shown in Fig. 1. In this case, three isolated bands closest to the Fermi level mainly consist of the $3d$ t_{2g} states, which defines the Hilbert subspace $\{|d\rangle\}$. Then, the equations for eigenvalues and eigenfunctions of the LDA Hamiltonian $\hat{H}$ can be rewritten as

$$(\hat{H}^{dd} - \omega)|d\rangle + \hat{H}^{dr}|r\rangle = 0, \quad (1)$$

$$\hat{H}^{rd}|d\rangle + (\hat{H}^{rr} - \omega)|r\rangle = 0. \quad (2)$$

We eliminate the subspace $|r\rangle$, which yields the effective ω-dependent Hamiltonian for only the d subspace: $\hat{H}^{dd}_{\rm eff}(\omega) = \hat{H}^{dd} - \hat{H}^{dr}(\hat{H}^{rr} - \omega)^{-1}\hat{H}^{rd}$. From the overlap matrix $\hat{S}(\omega) = 1 + \hat{H}^{dr}(\hat{H}^{rr} - \omega)^{-2}\hat{H}^{rd}$, with $\langle d|\hat{S}|d\rangle = 1$, the tight-binding effective Hamiltonian, $\hat{h}$ is obtained after the orthonormalization of the vectors $|d\rangle \rightarrow |\tilde{d}\rangle = \hat{S}^{1/2}|d\rangle$ and fixing the energy ω in the center of gravity of the band of our interest: $\hat{h} = \hat{S}^{-1/2}\hat{H}^{dd}_{\rm eff}\hat{S}^{-1/2}$. After Fourier transformation to the real space, $\hat{h}$ defines the *Wannier basis*. The band structure obtained after the elimination of the higher-energy bands shows an excellent agreement with the LDA band computed from the LMTO basis as we see in Fig. 1. This formalism has generality and can be easily extended to a more complex band structure [15].

We now derive an effective Coulomb interaction $\hat{W}_r$ among electrons at the isolated t_{2g} Wannier orbitals after considering the screening by other bands. In principle, $\hat{W}_r$ may be derived by a full GW scheme [6]. However, for practical use, the whole GW calculation requires large computation time. Since the screening from the polarizations of high-energy electrons does not have strong fluctuations, it may alternatively be replaced by the constrained-LDA (C-LDA) method [16]. Then we take two steps. First, we compute the interaction $\hat{W}_{r1}$ which takes into account the screening by the electrons residing at *atomic orbitals* other than $3d$. This step is performed by the C-LDA method [16]. When the higher-energy bands are well separated, we expect that the frequency dependence is small around the Fermi level and it may well be calculated by the C-LDA scheme [16] by starting with the basic definition of the effective Coulomb interaction formulated by Herring [17]: $U_{\mathbf{RR}'} = E[n_{\mathbf{R}} + 1, n_{\mathbf{R}'} - 1] - E[n_{\mathbf{R}}, n_{\mathbf{R}'}]$, which is nothing but the energy cost for moving a $3d$ electron between two atoms, located at $\mathbf{R}$ and $\mathbf{R}'$, and initially populated by $n_{\mathbf{R}} = n_{\mathbf{R}'} \equiv n$ electrons. Note that at this stage, the screenings of $3d$-$3d$ interactions by the electrons at the same $3d$ *atomic* orbitals are excluded, because the $3d$ atomic orbitals do not hybridize each other in a C-LDA scheme. For Sr_2VO_4, the on-site Coulomb interactions derived from $U_{\mathbf{RR}'}$ is $U \simeq 11.3$ eV. For comparison, the bare Coulomb interaction is 21.8 eV. Thus, the screening of $3d$-$3d$ interactions by non-$3d$ electrons is strong. In addition to U, the intra-atomic exchange coupling J can be easily calculated in the C-LDA approach. By using these two parameters, one can restore the full matrix $\hat{W}_{r1}$ of screened Coulomb interactions [18].

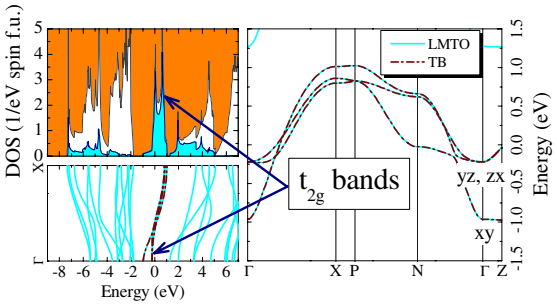

FIG. 1 (color online). (Left panel) Electronic structure of Sr_2VO_4 in LDA. (Right panel) Enlarged behavior of t_{2g} bands computed from LMTO basis functions (solid light blue curves) and downfolded tight-binding bands (dot-dashed brown curves). The corresponding bands in the left panel are shown by arrows. The symbols denote the character of t_{2g} bands in the Γ point. The Fermi level is at zero energy.

It is known that LDA does not take into account the self-energy effect and fails in reproducing a gap at the Fermi level [5]. LDA also ignores energy shifts in core levels arising from the self-interaction effect. However, in the present scheme, the bands near the Fermi level are left for a more refined PIRG method, while the core electrons hardly polarize and do not contribute to the screening. The valence electrons give the major contribution to the screening in this C-LDA treatment and their energies are well described by LDA with few self-energy corrections in many cases including transition-metal oxides [19]. Therefore, although C-LDA is not complete, it offers a reasonable and efficient way of counting the screening effects.

In the second step, we use the GW scheme [6] by taking $\hat{W}_{r1}$ as if it is the starting bare Coulomb interaction. Then the RPA screening produces $\hat{W}_r(\omega) = \hat{W}_{r1}/(1 - \hat{P}_{dr}(\omega) \times \hat{W}_{r1})$. The whole polarization of the $3d$ *atomic orbitals* in the LMTO basis is given by $\hat{P}_d(\omega) = \hat{P}_{dr}(\omega) + \hat{P}_{t2g}(\omega)$, where $\hat{P}_{t2g}(\omega)$ is the polarization purely from the t_{2g} *LDA band*, while $\hat{P}_{dr}$ represents the rest of the $3d$ *atomic orbitals* contribution contained in the e_g *LDA band* as well as in the component hybridized in the oxygen $2p$ *LDA band*. Since the identity $\hat{W}(\omega) = \hat{W}_{r1}/(1 - \hat{P}_d(\omega)\hat{W}_{r1}) = \hat{W}_r/(1 - \hat{P}_{t2g}(\omega)\hat{W}_r)$ holds, $\hat{W}_r$ plays the role of the effective interaction in the downfolded Hilbert space of the t_{2g} *LDA band*. We also note that some of the oxygen $2p$ LMTO component is contained in the $3d$ t_{2g} *Wannier orbital*. The screening by these components is already taken into account by the C-LDA scheme, while it should be excluded

in the low-energy model for the $3d$ t_{2g} *Wannier orbitals*. In practice, however, this contribution to the screening turns out to be negligible. Although the whole GW scheme considering P_{t2g} results in W, we consider the interaction within the t_{2g} LDA band more accurately by the low-energy solver as we explained above. Then in the effective low-energy model for the basis representation of the t_{2g} *Wannier orbital*, the screened Coulomb interaction is given by $\hat{W}_r$. In general, $\hat{W}_r$ becomes frequency dependent (Fig. 2). If the frequency dependence is small within the range of the t_{2g} bandwidth, we are allowed to take the low-frequency limit $\hat{W}_r(\omega = 0)$ as the interaction part $\hat{U}$ [6].

In the downfolding process, the kinetic-energy part is modified through the self-energy $\Sigma(k, \omega)$, which can be evaluated in the GW approximation [6]. Here the self-energy effect from $3d$ and $2p$ atomic orbitals is considered while the polarization of the higher-energy bands is small and we neglect it. We also take into account the self-energy arising from the dynamical part of the Coulomb interaction $\hat{W}_r(\omega) - \hat{W}_r(\omega = 0)$ through the GW scheme [6]. Such a self-energy effect mainly appears through $\mathrm{Re}\Sigma$, and contributes to the renormalization factor $Z = (1 - \partial\Sigma/\partial\omega)^{-1}_{\omega=0}$ ($\sim$0.8 for Sr_2VO_4). The low-energy part of $\mathrm{Im}\Sigma$ can be ignored (Fig. 2). Then the effective Hamiltonian is reduced to a multiband Hubbard model in the *Wannier representation* for the t_{2g} band:

$$\mathcal{H} = \sum_{\langle i,j\rangle m,m',\sigma} t_{ij}^{mm'} c_{im\sigma}^{\dagger} c_{jm'\sigma} + \frac{1}{2} \sum_{i,\alpha,\beta\gamma,\delta} U_{\alpha\beta\gamma\delta} c_{i\alpha}^{\dagger} c_{i\beta}^{\dagger} c_{i\gamma} c_{i\delta}, \quad (3)$$

where $c_{im\sigma}^{\dagger}(c_{im\sigma})$ creates (annihilates) an electron with the spin $\sigma = (\uparrow, \downarrow)$ at the t_{2g} Wannier orbital $m = (xy, yz, zx)$ of the site i and $n_{im\sigma} = c_{im\sigma}^{\dagger} c_{im\sigma}$. The Greek symbols stand for the combination (m, σ) of the indices.

We now discuss the PIRG method [12] as a solver of the low-energy effective Hamiltonian. The basic method is to perform the path integral by following the principle that $\lim_{p\to\infty}[\exp(-\tau\mathcal{H})]^p|\Phi\rangle$ generates the ground state, with a proper trial wave function $|\Phi\rangle$. The path integral is expressed by the summation over the Stratonovich variables after the Stratonovich-Hubbard transformation of the interaction. This generates increased number of nonorthogonal Slater-determinant basis functions as $|\Phi_L\rangle = \sum_{i=1}^{L} c_i|\phi_i\rangle$. Then the truncated basis with a fixed L is constructed by the optimization of c_i and $|\phi_i\rangle$. Linear extrapolation to the full Hilbert space as a function of the energy variance, obtained by a systematic increase of L, leads to an accurate estimate of the ground state. It is also crucial to implement a quantum-number projection in restoring the symmetry of the Hamiltonian [13]. A typical accuracy is seen in the energy estimate of $-1.85\,790 \pm 0.00\,002$ compared with the quantum Monte Carlo result of -1.8574 ± 0.0014 for the standard Hubbard model at half filling on a 6×6 square lattice with the transfer $t = 1$ at the interaction $U = 4$ [13].

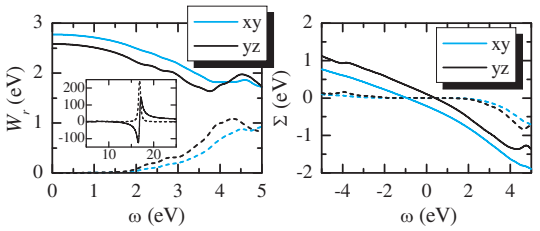

FIG. 2 (color online). Diagonal matrix elements of the screened Coulomb interaction $W_r(\omega)$ (left panel) and the self-energy, $\Sigma(\omega)$ (right panel). The inset shows the high-frequency part of $W_r(\omega)$ (the lines corresponding to the xy and yz orbitals are indistinguishably close). The real and imaginary parts are shown by solid and dashed curves, respectively.

The present first-principles method combined with the PIRG solver is now applied to calculate the electronic structure of Sr_2VO_4. This compound has a layered perovskite structure and bears a intriguing character because this has one $3d$ electron per V site (d^1 system) with strong two-dimensional anisotropy and has a dual relation to the one $3d$ hole per Cu sites (d^9 system) in the mother compounds of the cuprate superconductors. The duality is not complete because, in Sr_2VO_4, the orbital degeneracy of d^1 electrons remains perfectly between the d_{yz} and d_{zx} orbitals. The crystal field splitting of the d_{xy} orbital is also rather small ($\sim$0.08 eV in the LDA calculation).

In the case of Sr_2VO_4, after the downfolding, the on-site interactions among the Wannier orbitals of intraorbital xy, $yz(zx)$ and interorbital xy-$yz(xy$-$zx)$ and yz-zx combinations are $U = 2.77$, 2.58, 1.35, and 1.28 eV, respectively. The on-site exchange interactions between xy-$yz(xy$-$zx)$ and yz-zx orbitals are 0.65 and 0.64, respectively. The nearest neighbor transfers between xy-xy, yz-yz, and zx-zx orbitals in the x direction are -0.22, -0.05, and -0.19 eV, respectively. Although the next-nearest-neighbor transfers are considerably smaller, they have also been considered. In order to monitor the Coulomb interaction, we examine the scale-factor dependence by multiplying all the matrix elements $U_{\alpha\beta\gamma\delta}$ with a factor λ. Namely, the realistic value corresponds to $\lambda = 1$. The model (3) is solved by PIRG with sizes from 4×4 up to 8×4 and $4 \times 4 \times 2$ unit cells with the periodic boundary conditions, which confirms few size dependences. The above linear extrapolation is taken from the bases up to $L = 192$. Details will be reported elsewhere [20].

Sr_2VO_4 was experimentally studied by Cyrot *et al.* and Nozaki *et al.* [21,22] and recently thin film formed on $LaSrAlO_4$ was studied by Matsuno *et al.* [23]. Transport and optical properties indicate a very small Mott gap with rapidly increasing resistivity with decreasing temperature. It can be easily metallized by La doping [23]. The magnetic susceptibility appears to show presumable antiferromagnetic transition at around 50 K.

In sharp contrast to the nearly insulating transport properties, the LDA calculation predicts a good metallic be-

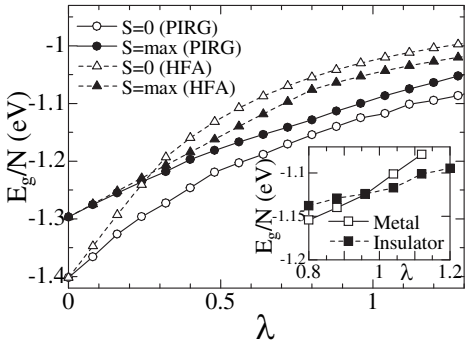

FIG. 3. Lowest energies per unit cell of total $S = 0$ (open symbols) and ferromagnetic states (filled symbols) by quantum-number projected Hartree-Fock (triangles) and PIRG (circles) calculations for the downfolded model of Sr_2VO_4. (Inset): Lowest energies per unit cell of metallic (open squares) and insulating states (filled squares) by quantum-number projected PIRG for the downfolded model of Sr_2VO_4.

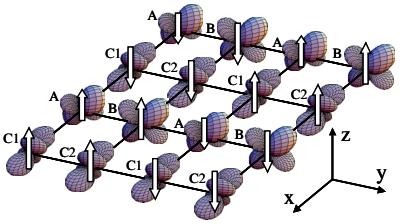

FIG. 4 (color online). Ordered spin-orbital patterns in plane for Sr_2VO_4. Ordered spin moment is proportional to the length of the arrows. At each site, occupied orbitals can be specified by a 3-dimensional unit vector in the basis of t_{2g} Wannier orbitals. Its xy, yz, and zx components are given by (0.70,0.60,0.39), (0.51,0.80,0.31), (0.40,0.04,0.92), and (0.33,0.06,0.94), for the sites A, B, C1, and C2, respectively.

havior (Fig. 1). On the other hand, the Hartree-Fock approximation (HFA) predicts a clear ferromagnetic insulating phase at the realistic parameter values (see Fig. 3). LDA + U approach [18] predicts similar results to HFA.

The PIRG results indicate that the ground state becomes close to the metal-insulator transition and total spin $S = 0$ in contrast to the HFA as in Fig. 3, but consistently with the experiment. The Mott transition occurs at $\lambda \sim 0.95$ as indicated in the inset of Fig. 3. Furthermore, the PIRG results in a nontrivial orbital-stripe long-period 2×4 structure as shown in Fig. 4. This is interpreted from the orbital degeneracies and long-range exchanges leading to frustration effects. It remains paramagnetic in the metallic side. The realistic relativistic spin-orbit coupling does not seem to alter the present conclusion [20]. Several possible interlayer configurations are degenerate within our accuracy (~0.005 eV). At least, the antiferromagnetic insulating state is consistent with the experiments, while the configurations of spin-orbital order are not experimentally available so far.

It has turned out that this compound shows very severe competitions. First, it lies on the verge of the Mott transition. Second, the ferromagnetic state is rather close in energy to the true ground state. Third, candidates of the spin-orbital order are in severe competition with each other in the order of 100 K. The available experimental results are consistent with our results, while the LDA, LDA + U, and Hartree-Fock are not. The failure of single-Slater-determinant approximations such as HFA and LDA + U is naturally understood because they relatively well describe a simple ferromagnetic state, while not the antiferromagnetic state with a nontrivial periodicity. Such a phase with large quantum fluctuations can be described only by our PIRG scheme going beyond a single-Slater determinant. All of the above indicate that our present approach of PIRG combined with the downfolding by using the LDA-GW scheme offers a promising computational method for strongly correlated electron systems. This compound offers a good benchmark for taking account correlation effects in computational methods.

The authors are grateful to F. Aryasetiawan for fruitful discussions and also thank Y. Tokura and J. Matsuno for clarifications of experimental results on Sr_2VO_4.

[1] P. Hohenberg and W. Kohn, Phys. Rev. **136**, B864 (1964).
[2] W. Kohn and L. J. Sham, Phys. Rev. **140**, A1133 (1965).
[3] W. Kohn, Rev. Mod. Phys. **71**, 1253 (1999).
[4] L. Hedin *et al.*, Solid State Phys. **23**, 1 (1969).
[5] F. Aryasetiawan *et al.*, Rep. Prog. Phys. **61**, 237 (1998).
[6] F. Aryasetiawan *et al.*, Phys. Rev. B **70**, 195104 (2004).
[7] I. V. Solovyev *et al.*, Phys. Rev. B **71**, 045103 (2005).
[8] A. Georges *et al.*, Rev. Mod. Phys. **68**, 13 (1996).
[9] For example, V. I. Anisimov *et al.*, J. Phys. Condens. Matter **9**, 7359 (1997); S. Y. Savrasov, G. Kotliar, and E. Abrahams, Nature (London) **410**, 793 (2001); K. Held *et al.* Phys. Rev. Lett. **86**, 5345 (2001); A. I. Lichtenstein *et al.* Phys. Rev. Lett. **87**, 067205 (2001).
[10] M. H. Hettler *et al.*, Phys. Rev. B **61**, 12 739 (2000).
[11] G. Kotliar *et al.*, Phys. Rev. Lett. **87**, 186401 (2001).
[12] M. Imada and T. Kashima, J. Phys. Soc. Jpn. **69**, 2723 (2000); T. Kashima and M. Imada, *ibid.* **70**, 2287 (2001).
[13] T. Mizusaki *et al.*, Phys. Rev. B **69**, 125110 (2004).
[14] O. K. Andersen, Phys. Rev. B **12**, 3060 (1975); O. Gunnarsson *et al.*, *ibid.* **27**, 7144 (1983).
[15] I. V. Solovyev, Phys. Rev. B **69**, 134403 (2004).
[16] P. H. Dederichs *et al.*, Phys. Rev. Lett. **53**, 2512 (1984).
[17] C. Herring, in *Magnetism*, edited by G. T. Rado and H. Suhl (Academic, New York, 1966), Vol. IV.
[18] I. V. Solovyev *et al.*, Phys. Rev. B **50**, 16 861 (1994).
[19] A. Yamasaki and T. Fujiwara, Phys. Rev. B **66**, 245108 (2002); J. Phys. Soc. Jpn. **72**, 607 (2003).
[20] Y. Imai, I. V. Solovyev, and M. Imada (unpublished).
[21] M. Cyrot *et al.*, J. Solid State Chem. **85**, 321 (1990); M. J. Rey *et al.ibid.* **86**, 101 (1990).
[22] A. Nozaki *et al.*, Phys. Rev. B **43**, 181 (1991).
[23] J. Matsuno, Y. Okimoto, M. Kawasaki, and Y. Tokura, Appl. Phys. Lett. **82**, 194 (2003); Phys. Rev. Lett. **95**, 176404 (2005).